J MATER SCI 41 (2006) 1145–1155

Substantiating the role of phase bicontinuity and interfacial bonding in epoxy-silica nanocomposites

LENO MASCIA*
Institute of Polymer Technology and Materials Engineering, Loughborough University, Loughborough, LE11 3TU, UK

LUCA PREZZI
SAFE Nanotechnology — Italia Srl, Via O. Belluzzi, 183e, 00128 Rome, Italy

BARRY HAWORTH
Institute of Polymer Technology and Materials Engineering, Loughborough University, Loughborough, LE11 3TU, UK

Published online: 4 February 2006

Nanocomposites consisting of an epoxy network matrix and a silica reinforcing phase were produced from a resin mixture functionalized with alkoxysilane coupling agents. Particulate nanocomposites were obtained by dispersing silica-organosol particles in the resin, while bicontinuous phase nanocomposirtes were obtained by the *in-situ* hydrolysis and condensation of tetraethoxysilane containing minor amounts of γ-glycidoxyl trimethoxysilane. Functionalization of the epoxy resin with an amine silane coupling agent was found to be more effective in aiding the dispersion of silica sol particles in the resin than the corresponding resin functionalized with a mercaptan silane coupling agent. Similar differences in the efficiency of coupling agent grafted on to the epoxy resin were observed for bicontinuous phase nanocomposites. The amine silane functionalization produces denser silica domains, which results in a higher rubber-plateau modulus and higher resistance to solvent penetration. The study also showed that the particulate nanocomposites are very ineffective in improving the solvent resistance of the base resin, even when the resin is grafted with a very efficient amine silane coupling agent, which promotes interfacial bonding. The different types of morphology were characterized by transmission electron microscopy and small angle X-ray scattering analysis.

1. Introduction

Materials consisting of nanostructured domains of an inorganic oxide interdispersed within an organic macromolecular compound are generally known as "organic-inorganic hybrids". The inorganic component is produced *in-situ* by the sol-gel method, starting from solution mixtures of metalalkoxides and either a polymer, or polymerizable monomers or network forming oligomers. In view of the interconnectivity of constituent inorganic oxide domains, organic-inorganic (O-I) hybrids can also be referred to as bicontinuous nanocomposites [1].

The formation of continuous inorganic glassy domains within the organic medium relies on establishing the appropriate kinetics for the hydrolysis and condensation reactions of the alkoxide precursor, together with an adequate level of interactions with the surrounding organic medium, and on the setting up of strong interactions between the precursor components, via H-bonds or covalent bonds [2–5]. This will ensure that the bicontinuity of phases, resulting from the chemically induced spinal decomposition of the inorganic oxide precursor, is maintained during the entire preparation procedure [6–8]. It is for this reason that bicontinuous nanocomposites with a hybrid organic-inorganic constitution are normally produced from tetra-alkoxysilanes, particularly tetraethoxysilane (TEOS) [9–10].

Nanocomposites containing particulate inorganic oxides, on other hand, are produced under conditions leading to fast rates of condensation reactions, so that phase separation takes place by a nucleation and growth mechanism. With tetra-alkoxysilanes these conditions are achieved by carrying out the sol-gel reactions in a basic environment,

*Author to whom all correspondence should be addressed.
0022-2461
DOI: 10.1007/s10853-005-3653-5

or in the presence of dibutyl tin dilaurate, so that the nucleation of inorganic oxide particles becomes the rate-determining step for their formation [11].

For the case of those metal alkoxides which produce crystalline inorganic oxides, such as titanium and zirconium alkoxides, nucleation-and-growth is the prevailing phase separation mechanism and, therefore, only particulate nanocomposites can be produced by the sol-gel method for organic–inorganic hybrids [12, 13].

The geometric configurations of nanocomposites makes it difficult to predict even basic properties, such as Young's modulus and coefficient of thermal expansion. For instance, the law of mixtures for predicting the Young's modulus along the direction of the fibres for unidirectional continuous fibre composites, cannot be applied to bicontinuous phase nanocomposites. The stipulated isostrain conditions within the two component phases would be invalidated by the geometric irregularities of the constituent phases, which set up spurious shear strains at the interfaces. Similarly any attempt to apply the Halpin – Tsai theory for predicting the modulus enhancement factor for discontinuous fibre composites would be facing insurmountable difficulties in determining the values for various constants required, such as contiguity factor and the adjustable constant ζ [14].

The aim of this study is provide experimental verifications of the influence of the geometrical configurations of the inorganic phase within an organic matrix on the physical properties of nanocomposites. These are assessed by measuring the dynamic mechanical properties, the thermo-mechanical properties and sorption properties of bicontinuous phase and particulate nanocomposites, using purposely functionalized epoxy resins and alkoxysilanes as the silica precursor through sol-gel reactions.

2. Experimental procedures

2.1. Materials

2.1.1. Resin

The resin used was a mixture of two bis-phenol A type epoxy resins, commercially known as Epikote 828, and Epikote1009, both obtained from Shell Chemicals. These have a number average molecular weight of 370 and 5000 atomic mass units respectively, corresponding to an average degree of polymerization of 0.1 and 16 expressed in terms of central $CH_2CHOHCH_2$ units per molecule. The general structure is as shown below:

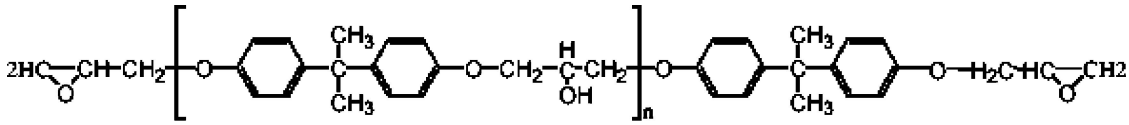

Bisphenol-A Epoxy Resin

On the basis of results obtained in previous work which showed that higher molecular weight resins produced a "better compatibility" of the two phases (i.e. finer domains), the weight ratio of Epikote 828 to Epikote 1009 used in the mixture was 6 : 1 in all cases [15].

2.1.2. Hardener

The hardener used in all cases was 4-4′ methylene bis-cyclohexaneamine (PACM), obtained from Air Products, as a 99% purity grade. The chemical structure is.

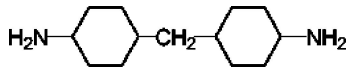

2.1.3. Coupling agents for functionalization of epoxy resin

The structure of the silane coupling agents used and the source are shown below:

Bis-(γ-propyltrimethoxysilane)amine (A1170) (OSi Specialities, >95 % purity)

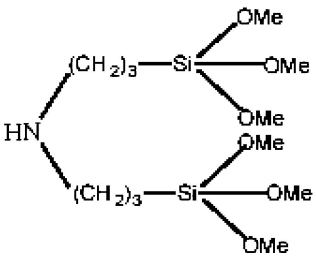

Mercapto γ-propyltrimethoxysilane (MPTMS) (AKCROS, >95 % purity)

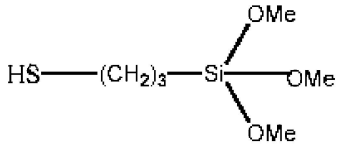

2.1.4. Precursors for the siloxane component

These were respectively tetraethoxy silane, as the main component (TEOS) and γ-glycidoxyl trimethoxysilane (GOTMS) as coupling agent. Both were obtained from ACROSS, purity > 95%.

(TEOS)

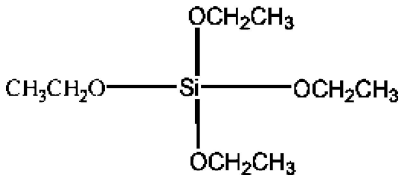

(GOTMS)

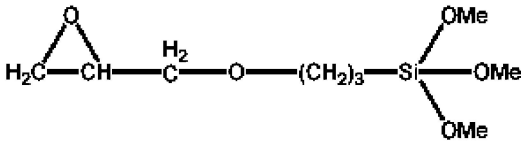

2.1.5. Catalysts for the alkoxysilane component

The catalyst was Dibutyl-tin-dilaurate (TIN), obtained from Aldrich, >95% pure.

2.1.6. Silica Organosol

This was obtained from Clariant as a 30% w/w silica microdispersion in isopropanol, sold under the trade name of Highlink OG 502-30. It contains silica primary particles with diameter in the region of 10–13 nm. The pH is claimed to be 2.8–4.0 after dilution in water to 10% solids.

2.1.7. Auxilaries

Solvents used were xylene (Fluka) and butanol (Aldrich).

2.2. Preparation procedures

2.2.1. Functionalization of the epoxy resin mixture

The epoxy resins were initially dissolved in a mixture of xylene and butanol (2:1). The composition of the solution was fixed at 60% solids to obtain a viscosity in the region of 1–2 Poise. The weight ratio of the epoxy resins was 85% Epikote 828 and 15% Epikote 1009. The grafting reaction with the silane coupling agent were carried out at molar ratio Epoxy : XH = 10 : 1, where X is N for amine and S for mercaptan silane, respectively. The details of the reactions have been described elsewhere [16].

Reaction scheme for the functionalization of the epoxy resin

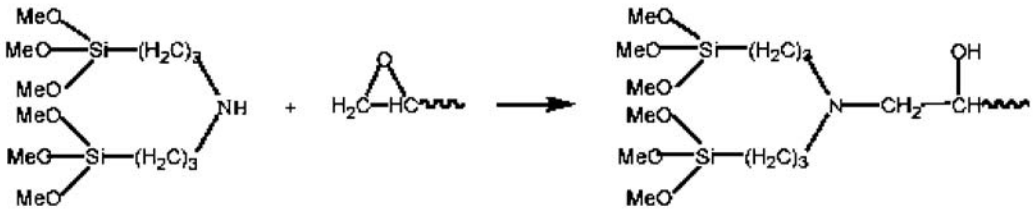

A1170 Epoxy resin Functionalised Epoxy resin

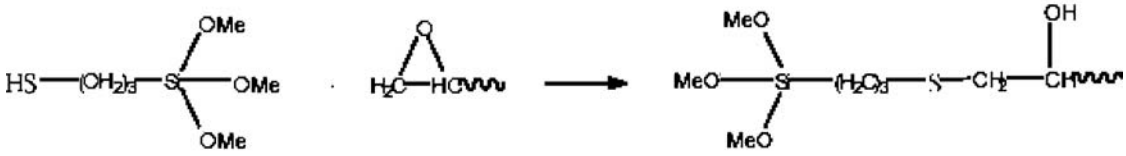

MPTMS Epoxy resin Functionalised Epoxy resin

2.2.2. Preparation of the silica precursor solution

Following the well established procedures used in similar work (12,15,16), TEOS, GOTMS, ethanol, water and TIN were mixed using the following molar ratios,

Water : TEOS = 3 : 1, Water : Ethanol = 1 : 1, TEOS : GOTMS = 1: 0.12.

In a previous study it was shown that the use of GOTMS in the alkoxysilane solution makes a notable contribution to the "compatibilization" of the silica domains with the epoxy resin matrix, even when the resin contains alkoxysilane functional groups [16].

The catalyst was added in amounts equal to 0.02% of the theoretical silica produced, including the equivalent

amount derived from the silane functional groups in the resin.

The Epoxy/TEOS weight ratios used were chosen to produce a nominal silica content of 15% w/w. The theoretical SiO_2 content was calculated from conversion of moles to weight quantities, from which it is estimated that 28.8% is derived from TEOS and 25.4% from GOTMS.

Cylindrical glass containers, 2 cm wide, were used in all case and heating was provided by a hot plate fitted with a magnetic stirring device. The silica precursor solution was stirred first for 5 min at room temperature, and then for 120 min at 90°C.

2.2.3. Production of epoxy-silica hybrids

After completion of the earlier described reactions, the components of the precursor solution were mixed with the epoxy resin in xylene/butanol solution and pre-reacted under stirring conditions for 15 min at 60°C and 120 min at 80°C.

2.2.4. Production of particulate nanocomposites

These were obtained by adding with magnetic stirring an amount of silica organosol to the epoxy resin mixture in xylene/butanol solution. This was carried out at room temperature for 5 min.

2.2.5. Specimen preparation and curing

The resin, the hybrid precursor solution and the hardener were mixed for 1 min at room temperature, and then spread on shallow moulds made from supported siliconized paper to produce small plaques about 0.5–1.0 mm thick. The amount of hardener was used in the following stoichiometric ratio Epoxy groups : -NH_2 groups = 1 : 0.375 (i.e 75% reactive NH_2 groups). Less than the stoichiometric amounts of hardener are required to reduce the extent of homopolymerization reactions, which bring about a reduction in cross-linking density [17].

The castings from the epoxy-siloxane hybrid mixture were left to gel and cure at room temperature for two days and were post-cured for 6 h at 80°C and then for a further 2 h at 120°C.

The same formulation details and preparation procedure was used to produce the particulate nanocomposites.

2.2.6. Characterization techniques

2.2.6.1. FTIR Analysis. Transmittance FTIR spectra were obtained using a Mattson 3000 spectrometer, with a resolution of 4 and 2 cm^{-1}, in the infrared spectra range 4000–600 cm^{-1}. Measurements were carried out by dispersing the powder samples in KBr to monitor the structure evolution of the siloxane domains and the state of cure of the epoxy matrix.

2.2.6.2. Transmission electron microscopy (TEM). The morphological structures of the O-I hybrids were characterized using a TEM-100CX apparatus, manufactured by JEOL Ltd. Examinations were made on thin slices microtomed from cast films embedded in epoxy resin.

2.2.6.3. Dynamic mechanical analysis. Dynamic mechanical tests were carried out on a DMTA Thermal Analyser from Polymer Laboratories (UK) model MK III. The samples were in the form of specimens ∼3 cm long, ∼5 mm wide and ∼1 mm thick. In these tests a sample clamped at the edges was subjected to a sinusoidal flexural deformation. A transducer detected the sample response to the applied load and by appropriate signal conditioning and data analysis, the instrument's software was used to calculate the viscoelastic constants of the material, namely the storage modulus (E′), and the dissipation factor (tan δ). The tests were performed in the scanning temperature mode from room temperature to 200°C at a constant rate of 5°C/min and with an oscillating frequency of 1 Hz.

2.2.6.4. Solvent absorption tests Specimens ∼20 mm long, ∼10 mm wide and ∼0.5 mm thick of the samples were immersed in THF (tetrahydrofuran) to determine the solvent absorption characteristics as a complementary evaluation of the nature of the networks. The weight of the samples was measured as a function of time and the weight increase was recorded on an analytical balance, after blot drying the specimen.

2.2.6.5. Thermal expansion. Thermo-mechanical tests were carried out using a DuPont 990 Thermal-Analyser. Samples were in the form of specimens 5 mm long, 5 mm wide and about 1 mm thick. During the test the specimens are heated at a constant rate of 10°C/min, from room temperature up to 150°C. A probe detects the linear expansion of the samples, across any chosen temperature range.

2.2.6.6. Small Angle X-ray Scattering. A point-beam Cu X-ray source was utilised for small X-ray scattering (SAXS) measurements in conjunction with a GADDS 2D detector from Bruker. The scattered beam intensity was plotted as a function of the variable q, which is defined as $q = 2\ (\sin\theta)/\lambda$, where θ is the scattered angle and λ is the wave-length of the X rays.

2.2.6.7. Thermogravimetric measurements. Thermogravimetric analysis was employed to estimate the actual silica content of the hybrid materials produced. Weight losses were measured with a Mettler TG50 thermobalance operating under air-flow. The samples were heated from room temperature to 750°C at a constant rate of 20°C/min.

3. Results

3.1. Curing reactions

The FTIR analysis has shown that there were appreciable quantities of epoxy groups present in both nanocomposite and O-I hybrids even after two days curing at room temperature. This was evidenced by the presence of absorption bands at around 1250 and 915 cm^{-1}, attributed to the bending of the C–H bond, and to the asymmetric stretching of the C–O–C bond of the epoxy group. After post-curing for 6 h at 80°C and 2 h at 120°C, the spectra revealed the complete disappearance of these absorption peaks and, therefore, the systems were deemed to have reached the required state of cure.

3.2. Formation of silica network

Following the procedure adopted by several workers [18, 19], the possibility of characterizing the silica network in the two types of systems was examined. According to these studies, the position of the infrared peak associated to the Si-O-Si asymmetric stretching of silica varies from ~1060 to ~1120 cm^{-1}, depending on the density of the silica. The lower the density of the silica (such as the silica of a sol-gel network) the lower is the wave-number associated with the relevant peak.

For the identification of the Si-O-Si stretching peak in the silica domains of the epoxy hybrids produced by the sol-gel, an amount of silica was produced by using the same silica precursors and curing conditions employed in the production of the epoxy-silica hybrids. The FTIR spectrum of these silica products is shown in Fig. 1. This clearly reveals the presence of a peak at 1077 cm^{-1} (diffuse silica) with a shoulder at ~1100 cm^{-1} (dense silica). Fig. 2 shows the FTIR spectra for the epoxy-silica hybrid (bicontinuous) nanocomposite and the corresponding filler-loaded (particulate) nanocomposite produced by the addition of pre-formed silica particles, after subtracting the base line spectrum of the epoxy resin matrix. These show a distinct Si-O-Si stretching peak at ~1108 cm^{-1} for particulate nanocomposites, confirming the "dense" nature of the silica used. The spectrum of the epoxy-silica hybrid (bicontinuous nanocomposite), shows the presence of a broad peak at around 1070 cm^{-1}, which is associated with the existence of a "diffused" silica network.

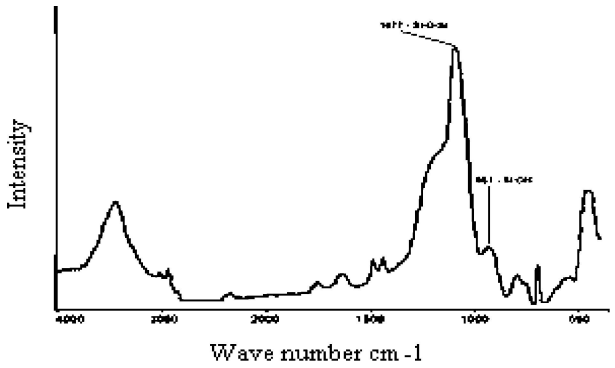

Figure 1 FTIR spectra of silica produced by the sol-gel method from the alkoxysilane precursor of epoxy-silica hybrids.

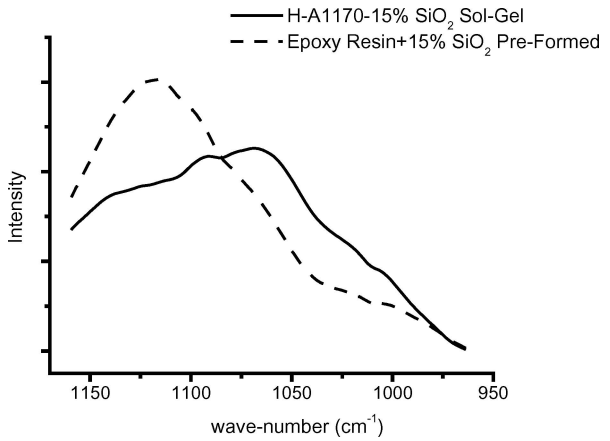

Figure 2 Comparison of FTIR spectra of epoxy-silica particulate nanocomposite (dotted curve) with epoxy-silica hybrid (continuous curve), both containing 15% w/w SiO_2, after subtracting the reference spectral line of the pure epoxy resin.

3.3. Morphological structure

The TEM examinations have revealed the presence of nanostructured bicontinuous domains for both functionalized resin systems. An example is shown in Fig. 3.

The micrographs of fractured surfaces indicate that the type of coupling agent (mercaptan-type or amine-type), used for the functionalization of the epoxy resin, exerts considerable influence on the dispersion of silica particles in the particulate nanocomposites.

When using a non-functionalized resin the sol nanoparticles form aggregates of secondary particles with diameter about 1–5 μm, as shown in Fig. 4. The level of agglomeration diminishes substantially when the epoxy resin is functionalized with MPTMS (Fig. 5 — left), but the silica aggregates are still large enough to produce optical opacity in the cured products. Complete dispersion of the silica particles was obtained, on the other hand, when the epoxy resin was functionalized with the amine coupling

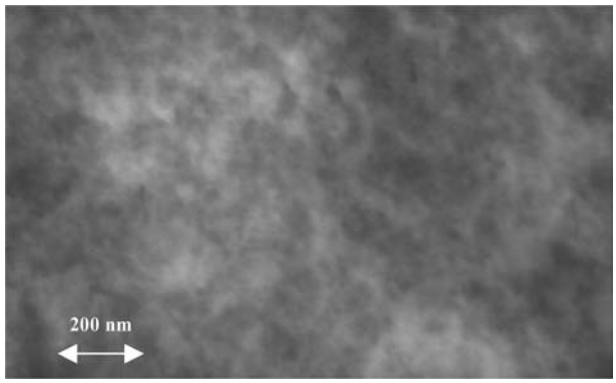

Figure 3 TEM micrograph of epoxy-silica hybrid (15% w/w SiO_2) produced from resin grafted with the amine silane coupling agent by the sol-gel method.

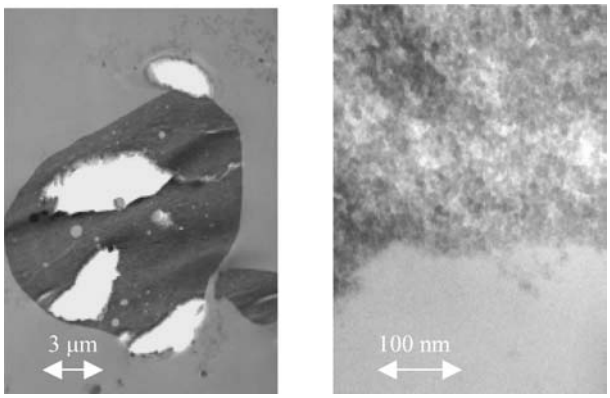

Figure 4 TEM micrographs of epoxy-silica nanocomposite (15% w/w SiO_2) produced from a mixture of unmodified epoxy resin and silica organosol.

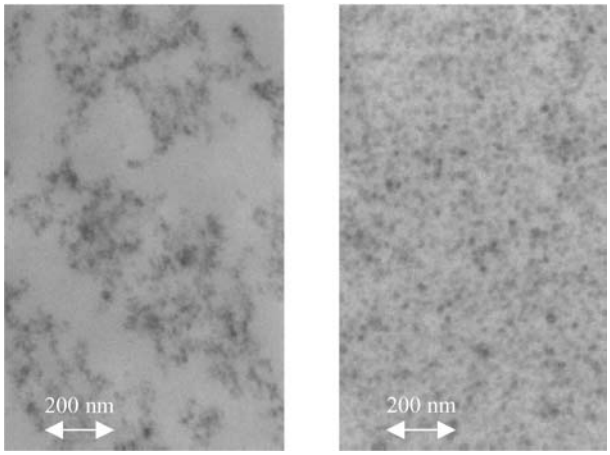

Figure 5 TEM micrographs of epoxy-silica nanocomposite (15% w/w SiO_2) produced from a mixture of silane grafted epoxy resin and silica organosol. A (left): Resin functionalized with the mercaptan silane coupling agent. B (right): Resin functionalized with the amine silane coupling agent.

agent (Fig. 5 - right). For these systems the TEM micrographs reveal a very fine morphology consisting of single isolated particles dispersed into the matrix.

3.4. Dynamic mechanical properties

The dynamic mechanical spectra in Fig. 6 show that the particulate nanocomposite produced with the unmodified epoxy resin displays much higher tan δ values in the rubbery plateau than the corresponding pure epoxy resin system, while the Tg remains almost unchanged within the range 80–83°C (tan δ values). The modulus curves are also very similar, except for a small increase in the rubber-plateau modulus for the particulate nanocomposite relative to the corresponding functionalized resin.

The dynamic-mechanical properties of the functionalized epoxy resin with A1170 (amine-type) and MPTMS (mercaptan-type) coupling agents, containing 15% w/w silica nanoparticles, are shown in Figs 7 and 8 and are compared with the equivalent bicontinuous nanocomposites. The tan δ data of both particulate nanocomposites, when compared to the corresponding functionalized epoxy system without the filler, reveal an increase in glass transition temperature of about 12°C for the resin functionalized with the mercaptan silane (MPTMS) coupling agent (Fig. 8), and 20°C for resin systems functionalized with the amine silane (A1170) coupling agent (Fig. 7). However, the elastic modulus curves show a reduction in the rubber-plateau values for nanocomposites produced from both types of functionalized resins, which can only be attributed to a reduction in the cross-linking density of the epoxy resin. This effect can only occur if a quantity of amine hardener is adsorbed on the surface of nanoparticles, making it less available for the cross-linking of the epoxy resin matrix. The much lower reduction in plateau modulus for systems based on amine silane functionalized resin (Fig. 7) is likely to be due to the larger number of alkoxysilane functional groups present at a given site, which counteracts the surface adsorption effect.

On the other hand, the bicontinuous nanocomposites produced with the resin functionalized with the amine silane coupling agent [coded H-A1170-15% SiO_2 (sol-gel)] show a lower and broader tan δ peak and higher plateau modulus, relative to the reference resin, although the Tg remains approximately unchanged. The same

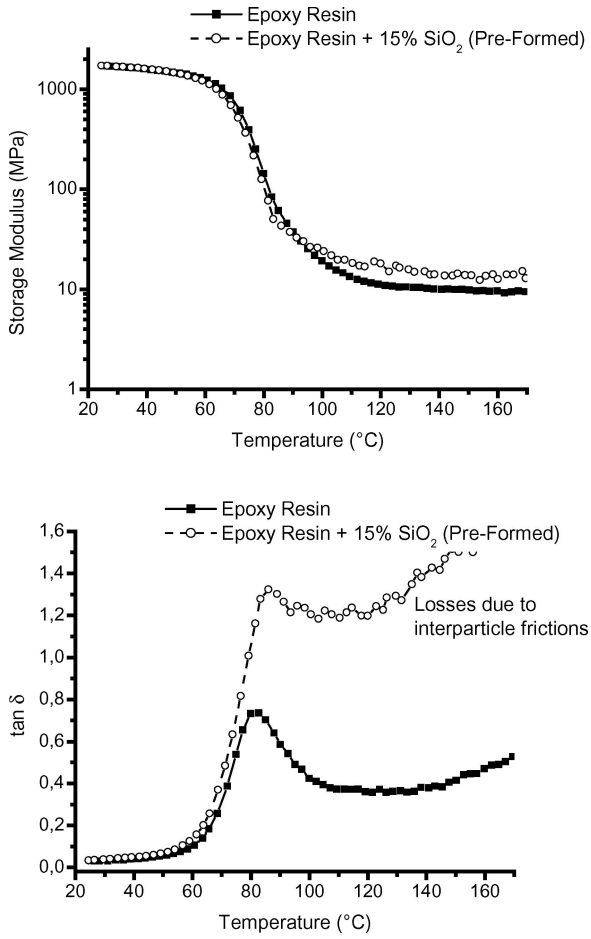

Figure 6 Dynamic mechanical spectra of unmodified epoxy resin and corresponding particulate nanocmposite (15% w/w SiO_2).

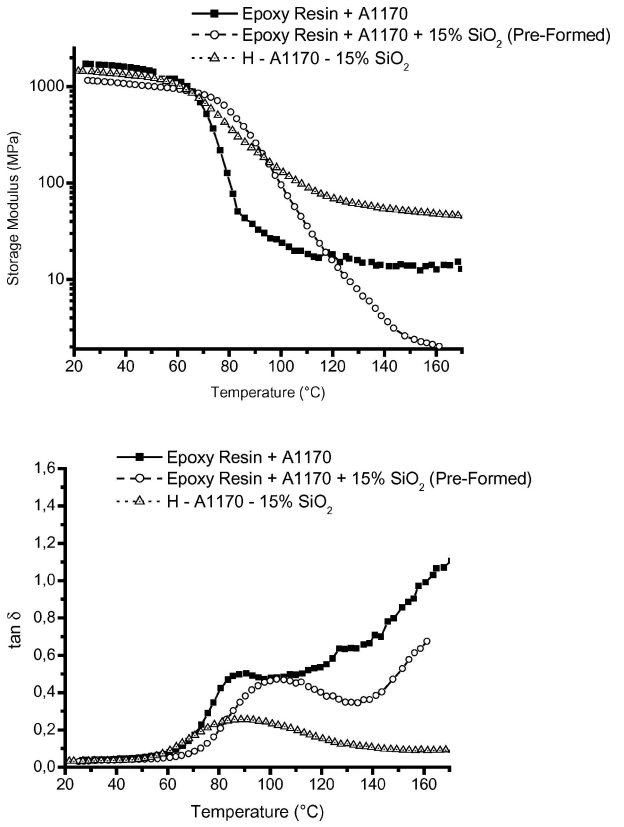

Figure 7 Comparison of dynamic mechanical spectra of amine silane functionalized epoxy resin (Epoxy Resin + A1170) with corresponding epoxy-silica particulate nanocomposite (Epoxy Resin + A1170 + 15% SiO_2 Pre-formed) and epoxy-silica hybrid (Epoxy Resin + H-A1170 + 15% SiO_2), both containing 15% w/w SiO_2.

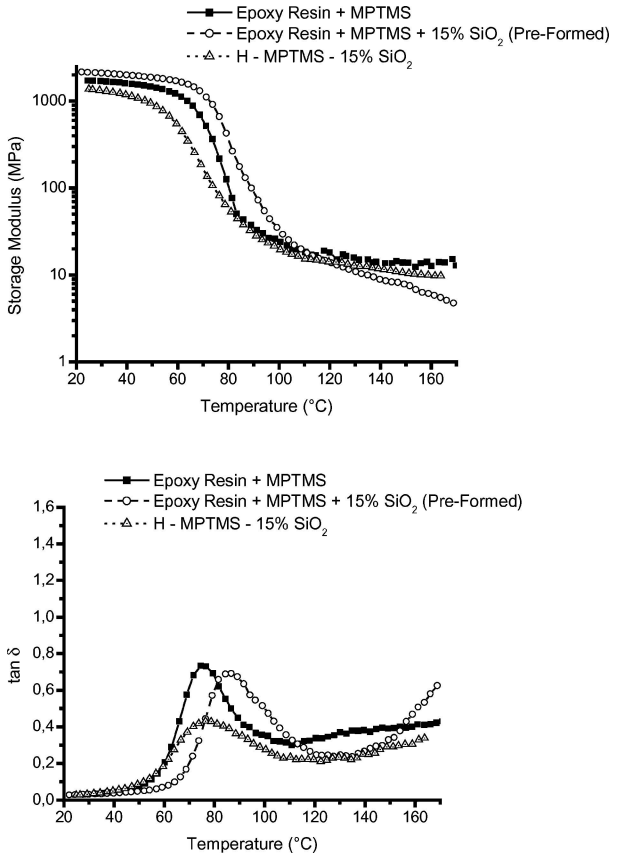

Figure 8 Comparison of dynamic mechanical spectra of mercaptan silane functionalized epoxy resin (Epoxy Resin + MPPTS) with corresponding epoxy-silica particulate nanocomposite (Epoxy Resin + MPPTS + 15% SiO_2 Pre-formed) and epoxy-silica hybrid (Epoxy Resin + H-MPPTS + 15% SiO_2), both containing 15% w/w SiO_2.

behaviour was observed with nanocomposites obtained from the resin functionalized with the mercaptan silane coupling agent. These results show that the silica formed in-situ by the sol-gel method (in the production of the O-I hybrids) creates strong constraints on the molecular motions within the organic phase. These constraining forces do not exist when the silica is added to the epoxy matrix as pre-formed particles, despite displaying a higher Tg. At the same time the silica reduces the cross-linking density, which is manifested as a reduction in the plateau modulus of the rubbery state (see Discussion).

The thermal expansion curves in Fig. 9 show that the thermal dilational behaviour of the particulate nanocomposite [coded Epoxy Resin-A1170+15% SiO_2 (pre-formed)] is very similar to that of the parent silane functionalized epoxy resin [coded Epoxy Resin-A1170]. Both show a large discontinuity between 80°C and 120°C. This is associated with relaxations within the organic phases and, therefore, corresponds to the Tg of the epoxy matrix. The thermal expansion curve for the bicontinuous nanocomposite [coded H-A1170-15% SiO_2 (sol-gel)], on the other hand, is very different. In this case the discontinuity almost disappears and the expansion exhibited by the epoxy matrix above the Tg is suppressed. This feature is in accordance with the previous interpretation of constraints to the molecular motions in the organic phase, due to restrictions imposed by the intermingled inorganic domains.

3.5. Solvent absorption behaviour

Fig. 10 shows a comparison of the THF absorption behaviour of the amine silane functionalized epoxy resin [coded Epoxy Resin-A1170], the corresponding particulate nanocomposite [coded Epoxy Resin-A1170-15% SiO_2 (pre-formed)], and bicontinuous phase nanocomposite [coded Epoxy Resin H-A1170-15% SiO2 (sol-gel)]. The data indicate that the higher resistance to swelling is obtained when the inorganic phase is bicontinuous with the organic network.

The linear increase in solvent uptake with time in the initial stage is synonymous with Case II diffusion, while the linear absorption followed by a sudden jump has been called Super Case II diffusion [25]. The detailed interpretation of such a peculiar solvent absorption behaviour for the present systems is discussed elsewhere [27].

Fig. 11 shows a comparison of the THF absorption behaviour of the epoxy resin functionalized with the mercaptan silane coupling agent [coded Epoxy Resin-

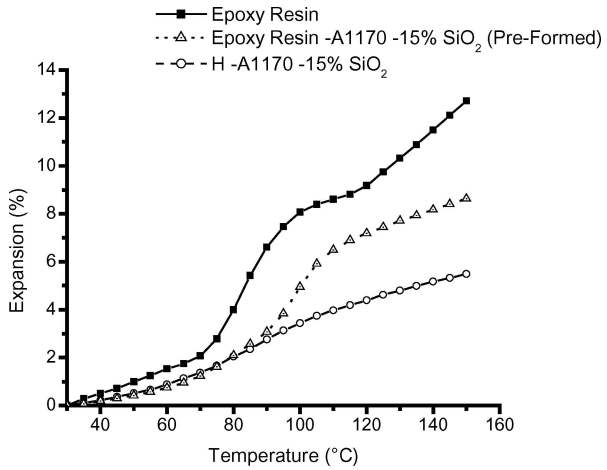

Figure 9 Comparison of linear thermal expansion variation with temperature of amine silane functionalized epoxy resin (Epoxy Resin) with corresponding epoxy-silica particulate nanocomposite (Epoxy Resin + A1170 + 15% SiO_2 Pre-formed) and epoxy-silica hybrid (Epoxy Resin + H-A1170 + 15% SiO_2), both containing 15% w/w SiO_2.

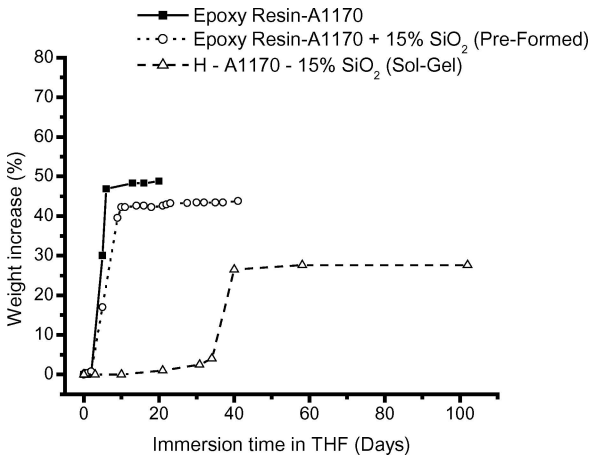

Figure 10 Comparison of solvent absorption behaviour of amine silane functionalized epoxy resin (Epoxy Resin + A1170) with corresponding epoxy-silica particulate nanocomposite (Epoxy Resin + A1170 + 15% SiO_2 Pre-formed) and epoxy-silica hybrid (Epoxy Resin + H-A1170 + 15% SiO_2), both containing 15% w/w SiO_2.

MPTMS], the corresponding particulate nanocomposite [coded Epoxy Resin-MPTMS-15% SiO_2 (pre-formed)], and the bicontinuous phase nanocomposite [coded H-MPTMS-15% SiO2 (sol-gel)]. These graphs show that only the bicontinuous phase nanocomposite H-MPTMS-15% SiO_2 (sol-gel) is resistant to solvent aggression. The other two samples, respectively plain functionalized resin {Epoxy Resin-MPTMS] and corresponding particulate nanocomposite [Epoxy Resin-MPTMS-15% SiO_2 (pre-formed)], not only displayed a very fast rate of solvent absorption but also disintegrate within a few hours before reaching the swelling equlibrium.

It is worth noting that the samples based on the mercaptan silane functionalized resin do not exhibit an induction time in the solvent absorption curve. This can be attributed to the lower cross-linking density, which also leads to a

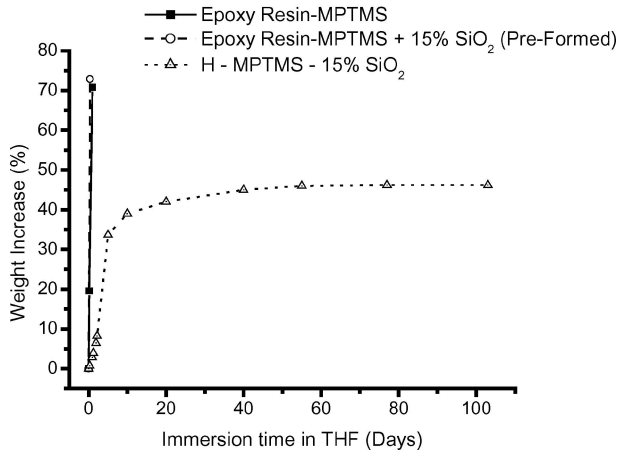

Figure 11 Comparison of solvent absorption behaviour of mercaptan silane functionalized epoxy resin (Epoxy Resin – MPPTS) with corresponding epoxy-silica particulate nanocomposite (Epoxy Resin + H-MPPTS + 15% SiO_2 Pre-formed) and epoxy-silica hybrid (Epoxy Resin + H-MPPTS + 15% SiO_2), both containing 15% w/w SiO_2.

"more open" surface structure for the immobilization of adsorbed solvent molecules.

3.6. Small angle X-Ray scattering.

Fig. 12 shows the X-Ray scattered intensities of the cured pure epoxy resin and the epoxy resin grafted with the amine coupling agent A1170. The plots represent in double logarithmic scale the scattered intensity versus the vector q ($q = 2 \sin \theta/\lambda$ [$Å^{-1}$]). The data for both samples show the presence of a peak at 63 Å, but it is unlikely to be due to any real structural features. It is more likely to be associated with some artifact in so far it appears within in domain spacings that are not normally associated with light scattering phenomena.

In Fig. 13 are compared the X-Ray scattered intensities for the particulate nanocomposites [coded Epoxy Resin-A1170-15% SiO_2 (pre-formed)] and the bicontinuous nanocomposite [coded Epoxy Resin H-A1170-15%

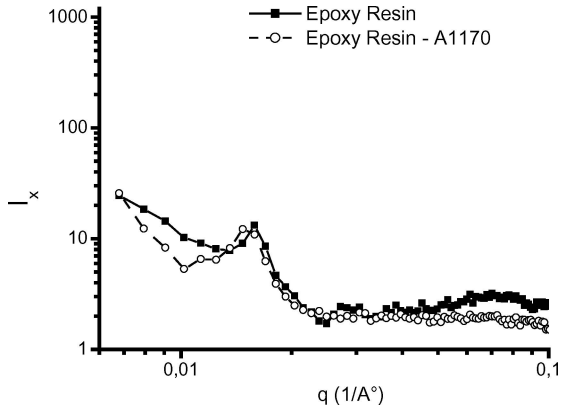

Figure 12 SAXS scattering profiles of pure epoxy resin (Epoxy Resin) and epoxy resin functionalized with the amine silane coupling agent (Epoxy Resin – A1170).

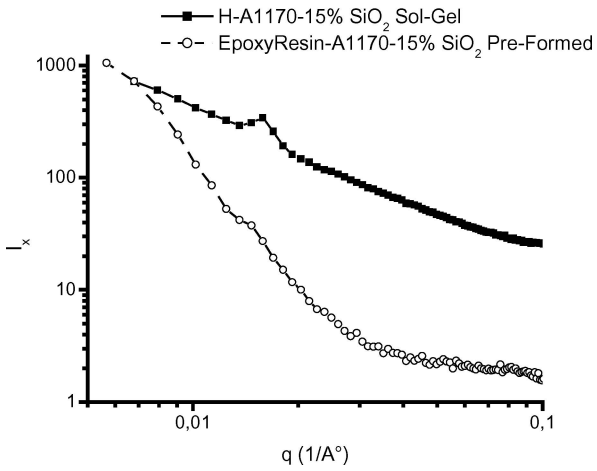

Figure 13 SAXS scattering profiles of epoxy-silica particulate nanocomposite (Epoxy Resin – A1170 + 15% SiO_2 Pre-formed) and epoxy-silica hybrid (Epoxy Resin – A1170 + 15% SiO_2 Sol-Gel), both based on the amine silane functionalized epoxy resin and both containing 15% w/w SiO_2.

SiO_2 (sol-gel)], both produced from the resin mixture functionalized with the amine coupling agent and containing 15% w/w nominal silica.

4. Discussion

4.1. Dispersion of silica-sol particles

From an inspection of the micrographs in Fig. 4 it is evident that, for systems produced from the non-functionalized epoxy resin, the individual nanoparticles within the agglomerated microparticles are weakly bound together by electrostatic forces. This is witnessed by a very large increase in tan δ above the glass transition temperature (Fig. 6).

When the resin is functionalized with the amine silane coupling agent (A1170) the positive surface charges on the surface of the nanoparticles, resulting from the acidic nature of the organosol used, can attract the grafted amine groups within epoxy resin, causing the SiO_2 nanoparticles to be thoroughly dispersed within the surrounding epoxy resin. At the same time the higher localized concentration of methoxy silane groups may also play a role in providing stronger interactions with the surface silanol groups of the silica-sol particles through a dynamic ester-exchange exchange equilibrium.

These conditions are less favourable when the epoxy resin is functionalized with the mercaptan silane due to lower attraction forces between the surface of the particles and the epoxy resin. This interpretation is based on considerations of relative proton acceptance character of the alkoxysilane grafted groups in the two cases. The sulphide groups derived from the mercaptan silane functionalization are weaker proton acceptors than the equvalent tertiary amine groups derived from the amine silane functionalization reaction.

For both systems, however, the alkoxysilane functionality in the epoxy resin is also expected to play a role in the dispersion of the nanoparticles, primarily with respect to the stabilization of the dispersion of the particles after the disintegration of the agglomerates. This is an entropic effect arising from the dynamic equilibrium in the exchanging of alkoxy groups between those on the surface of the particles and those grafted in on the epoxide chains. In this respect the higher concentration of alkoxysilane groups derived from the amine silane functionalization is expected to provide a more effective particle dispersion environment than the corresponding systems derived from the mercaptan silane functionalization of the resin, and will remain at the interface after curing the resin.

The internal plasticization caused by the pendant alkoxysilane in the epoxide chains, on the other hand, brings about a reduction in the rubber-plateau modulus. This is more pronounced for the case of systems produced from the amine silane functionalized resin, owing to the large amounts of such groups grafted onto the epoxy oligomer chains.

At the same time, the basic nature of the amine silane functionalized epoxy resin brings about an increase in the glass transition temperature, as a result of a higher cross-linking density and stronger interfacial bonding (compare the data in Fig. 7 with those in Fig. 9).

Accordingly the particulate nanocomposites produced from the amine silane functionalized epoxy resin display a considerably better resistance to solvent aggression than the corresponding system based on the mercaptan silane functionalized resin (compare the data in Fig. 10 with those in Fig. 11).

The decrease in the values of the rubber-plateau modulus (Figs 7 and 8) of the particulate nanocomposites produced from both functionalized resins, relative to rubber-plateau modulus values displayed by the parent epoxy resin, has to be attributed to the immobilization of the PACM hardener by the very high surface area of the nanoparticles. A reduction in the rubber-plateau modulus, on the other hand, is not observed for the case of particulate nanocomposites produced from the unmodified epoxy resin, owing to the much lower accessible surface area of the agglomerated particles.

4.2. Phase continuity and interconnectivity

While the TEM micrographs have provided a good indication of the morphological state of the different nanocomposites produced, the strongest evidence for the existence of bicontinuity between the organic and inorganic networks in epoxy-silica hybrids comes from small angle X-ray studies. The first observation for the scattered intensity diagrams is the existence of a peak at around 63 Å, which is evident in all the SAXS spectra obtained in these systems and is considered to correspond to an artifact in the measuring system used.

Two other observations on the scattering curves are relevant: (a) The scattering intensity of the sol-gel epoxy-silica hybrids (bicontinuous nanocomposites) has a linear dependence on the q function. (b) The slope of the X-ray

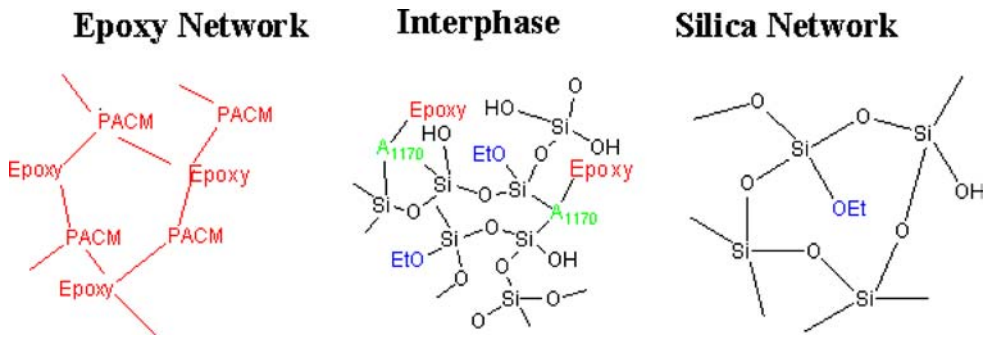

Figure 14 Composition of the constituent domains of epoxy-silica nanocomposites for systems derived from the resin functionalized with the amine silane coupling agent.

scattering curves varies between 1.1 and 1.3 for the case of the epoxy-silica hybrids produced, and is equal to 3.8 for the particulate nanocomposites which were obtained by the direct incorporation of preformed silica-sol particles. According to other reports [20–22] the linear change of the scattered intensity with q is indicative of the fractal nature of O-I hybrids produced by the sol-gel method. The slope of the curves, known as the fractal dimension (FD), is within the range of 1 and 3 when the phases are bicontinuous, and varies between 3 to 4 for phase separated structures. The values obtained for the systems of the present study lay in the extremes of these ranges, which is indicative of the presence of well segregated, sharply interfaced, domains for the case of particulate nanocomposites, and highly diffused domains in the case of bicontinuous nanocomposites produced by the sol-gel method. In particular the latter may be envisaged as being constituted of three domains, comprising an epoxy networks, a hybrid interphase and a silica network, as depicted in Fig. 14.

The type of alkoxysilane functionalization of the epoxy resin affects the relative ratio of these three components, particularly the ratio of silica/interphase domains. This ratio is larger for systems obtained from the resin functionalized with the amine silane coupling agent (A1170) than for those derived from the mercaptan silane (MPTMS) functionalized resin. These differences are reflected in all the physical properties measured. The lower Tg and lower rubber-plateau modulus revealed by dynamic mechanical tests for the systems based on the MPTMS functionalized resin (Figs 7 and 8) can be clearly attributed to the presence of a larger proportion of the interphase component. A similar deduction can be made with respect to the solvent absorption characteristics.

It is well known that when immersed in a good solvent an organic network will swell until it reaches equilibrium [23–25]. This is determined by the balance between the osmotic pressure generated by the penetration of the solvent and the constraining forced encountered by the stretching of the polymeric network.

In the case of particulate composites, if the particles are not bonded to the epoxy network they are unable to restrict the swelling of the polymer network and, therefore, they will not bring about any appreciable changes in solvent absorption resistance. If strong chemical bonds are formed at the interface of the particles and the epoxy network, on the other hand, some local constraints are produced to the stretching of the network, which will result is some improvement in solvent resistance.

Although some complications may arise from possible differences in local cross-linking density of the epoxy network near the particle surface, the data on solvent absorption for the particulate nanocomposites examined in the present study indicate that stronger interfacial bonds exist for systems based on the amine silane functionalized resin, than for those based on the mercaptan silane functionalized resin.

When the silica is present in the form of bicontinuous interpenetrating domains and interphases (as in the case of the *in-situ* generated silica), which are obviously covalently bonded to the epoxy matrix, the reduction in swelling is much more pronounced due to much higher constraints imposed on the stretching of the neighbouring organic network

The higher resistance to solvent penetration exhibited by the systems produced from the amine silane functionalized resin can, again, be related to higher silica/interphase ratio resulting from the high localized concentration of methoxysilane groups in the resin.

5. Conclusion

1. The dispersion of silica-organosols in an epoxy resin can be enhanced by the introduction of alkoxysilane groups in the resin through grafting reactions with suitable silane coupling agents. Functionalization of the epoxy resin with an amine silane coupling agent is more effective for this purpose than an equivalent functionalization with a mercaptosilane coupling agent.

2. Particulate nanocomposites provide only marginal improvements in solvent resistance over the parent resin matrix, even when the silica particles are thoroughly dispersed in the epoxy matrix and are chemically bonded to the matrix.

3. Both epoxy-silica nanocomposites produced by the sol-gel process from silane functionalized resin and

mixtures of tetraethoxysilane and minor amounts of γ-glycidoxyltrimethoxysilane coupling agent exhibit a bicontinuous phase morphology. This comprises three components, respectively an epoxy matrix network, a diffused silica phase and epoxy-silica interphase domains containing a prevalence of alkoxysilane components from the coupling agents used in the epoxy resin and tetraethoxy silane precursors.

4. Nanocomposites with a bicontinuous phase morphology exhibit large improvements in solvent resistance, the extent of which depends on the type of alkoxysilane used for the functionalization of the resin. The use of an amine silane coupling agent for the functionalization of the epoxy resin is more effective than the corresponding functionalization with a mercaptan coupling agent, for the enhancement of solvent resistance. This is attributed to the formation of denser siloxane domains, consisting of silica and silica-epoxy interphases.

Acknowledgements

The authors are grateful to International Coatings (Akzo Nobel), and to the Engineering and Physical Sciences Research Council, for providing the funds to carry out this work.

References

1. L. MASCIA, *Trends in Polymer Science* **3** (1995) 61.
2. M. R. LANDRY, B. K. COLTRAN and C. J. T. LANDRY, *J. Polym. Sci. Polym Phys.* **33** (1995) 637.
3. H. H. WANG, B. ORLER and G. L. WILKES, *Macromolecules* **20** (1987) 1322.
4. B. M. NOVAK, *Adv. Mat.* **5** (1993) 43.
5. J. J. FITZGERALD, C. J. T. LANDRY and J. M. POCHAN, *Macromolecules* **23** (1992) 3715.
6. A. KIOUL, L. MASCIA, *J. Non-Cryst. Solids* **175** (1994) 169.
7. L. MASCIA and A. KIOUL, *Polymer* **36** (1995) 3649.
8. Y. MORIKAWA, M. IYOKU, M. KAKIMOTO, Y. IMAI, *Polym. J.* **24** (1992) 107.
9. Z. AHMAD, S. WANG and J. E. MARK, *Polym. Prep.* (*Am. Chem. Soc., Div. Polym. Sci.*) **34**(2) (1993) 745.
10. J. F. CHEN, Z. AHMAD, S. WANG, J. E. MARK and F. E. ARNOLD, in "Hybrids Organic- Inorganic Composites" edited by J. E. Mark, C. Y-C Lee and P. A. Bianconi, (ACS Symposium Series 585, 1995) Chapter 23, p. 297.
11. E. P. BLACK, T. A. ULIBARRI, G. BEAUCAGE, D. W. SCHAEFER, R. A. ASSINK, D. F. BERGSTROM, P. A. GIWA-AGBOMEIRELE and G. T. BURNS, *Ibid* Chapter 18, pp 235-246.
12. J. WEIN, J. M. BREINER, J. E. MARK, Polymer **39** (1998) 5483.
13. S. S. SOUSA, A. N. FALCAO, M. CARRAPICO, F. M. MARCAGA, I. G. CARVALHO, S. SALVADO and J. TEIXEIRA, *J. Sol-Gel Science and Tech.* **26** (2003) 345.
14. J. E. ASHTON, J. C. HALPIN, P. H. PETIT, Primer on Composite Analysis (Tecnicon Publishing Co. Stanford, Conn. 1969) Chapter 5.
15. L. MASCIA and T. TANG, *J. Mat. Chem.* **8** (1998) 2417.
16. L. PREZZI and L. MASCIA, *Advances in Polymer Technology* **24** (2005) 91.
17. L. PREZZI, Ph. D. Thesis, Loughborough University, 2004.
18. C. J. BRINKER and G. W. SCHERER, *Sol-Gel Science: The Physics and Chemistry of Sol-Gel Processing*, Academic Press, London (1996).
19. A. KASGOZ and Y. ABE, *J. Sol-Gel Sci. and Tech.* **17** (2000) 127.
20. G. L. WILKES, B. ORLER and H. H. WANG, *Polymer Preprints* **26**(2) (1985) 300.
21. L. MATEJEIKA, K. DUSEK, J. PLETSIL, J. KRIZ and F. LEDNICKY, *Polymer* **40** (1998) 171.
22. B. BAUER, W. LIU, C. JACKSON, J. BARNES, *Polymers for Advanced Technologies* **7** (1995) 333.
23. C. M. HANSEN and L. JUST, *Ind. Eng. Chem. Res.* **40** (2001) 21.
24. C. M. HANSEN, *Polymer Degradation and Stability* **77** (2002) 43.
25. A. F. M. BARTON, Handbook of Solubility Parameters (CRC Press, 1971).
26. L. MASCIA, L. PREZZI and M. LAVORGNA, *Polym. Eng. Sci.* **45** (2005) 1039.

Received 16 June 2004
and accepted 25 May 2005